Interactions between vortices and flexible walls

Silas Alben

School of Mathematics, Georgia Institute of Technology, 686 Cherry Street, Atlanta, GA 30332-0160

Abstract

We give two fundamental solutions for the motion of a point vortex near a flexible wall, up to first order in wall deflection, using computational methods. For a point vortex near an infinite horizontal wall, the deformation of the wall intensifies the flow at the wall near the vortex, and increases the speed of the vortex. Near a circular wall there is a strong mutual amplification of the deflection of the wall and the pressure force induced by the deflection, as the point vortex approaches the wall. The total force on the wall diverges as the inverse cube of the distance to the point vortex, and the induced speed of the point vortex diverges as the inverse fourth power of distance to the wall.

Key words: Fluid, Vorticity, Flow, Vortex sheet, Bending

PACS: 47.11.-j, 47.11.Kb, 47.32.C-, 47.15.ki, 46.40.Jj

Email address: alben@math.gatech.edu (Silas Alben).

1 Introduction

The interaction of vortices with solid walls is a classical problem in hydrodynamics [1], with recent applications in problems of biological and technological interest. Doligalksi *et al.* [2] review studies of flows past aircraft and submarines where vorticity shed from upstream structures (i.e. airframes and helicopter blades) collides with downstream surfaces, causing boundary layer separation and leading to dramatic changes in unsteady forces. Rockwell's review [3] gives many additional examples including vortices impinging on small bodies, leading edges, and oscillating bodies, in the presence of three dimensional effects and nonuniform background flows. Many important vortex-body interactions occur in biological flows, both internal (heart flows [4]) and external (insect flight [5–7] and fish swimming and schooling [8,9]). Many of these biological structures undergo large deformations under forces induced by vortices. The goal of the present work is to obtain two of the most basic solutions for vortices interacting with deformable walls. These solutions can be regarded as a starting point for a wider class of interactions of vortices with flexible walls which incorporate boundary layer interactions, different vorticity distributions such as dipoles, and more complex geometries. Interactions of vorticity with passive flexible flag-like structures has also been studied experimentally [10], theoretically, and computationally [11–14].

We consider a two-dimensional flow consisting of a single point vortex translating along a flexible wall which is either an infinite line or a circle in the undeformed state. We solve the problem in the asymptotic limit of small deformations. For large deformations, boundary layer separation is likely, which would inject additional vorticity into the outer flow. The leading order wall de-

formation can be determined from the unperturbed flow, which can be solved using classical methods such as the method of images [1]. To understand how the wall deformation alters the motion of the vortex and the force on the wall, we use a more general formulation in terms of bound vortex sheets. We find that the wall deformation increases the speed of the vortex as it travels along the wall, and increases the force on the wall near the vortex. The total force on the wall is either unchanged (for the infinite wall) or increased (for the circular boundary) by the wall's deformation. As the distance between the point vortex and the circular wall is decreased, the first-order correction to the flow grows rapidly, due to a mutual amplification of the body's deformation and the fluid forces on the wall.

2 Point Vortex Near a Flexible Wall

We first give the equations for the motion of a single point vortex immersed in an inviscid fluid above an infinite flexible wall. The position ζ of the wall in the complex plane is given by its vertical deflection h from the horizontal axis, $\zeta(x,t) = x + ih(x,t)$ (see figure 1a). In what follows, we assume $h(x,t)$ is small compared to the length scale of the problem, which is the distance of the point vortex from the wall, d. Then we retain terms up to linear order in h and $\partial_x h$ and drop terms which are $O(h^2, \partial_x h^2)$. Some of the details of this expansion are given in [15,16]. The method given here can also be used for more general $\zeta(x,t)$.

The boundary condition that the flow does not penetrate the wall can be satisfied by placing a vortex sheet at the wall, which induces a normal velocity along the wall. The vortex sheet also induces a tangential velocity along the

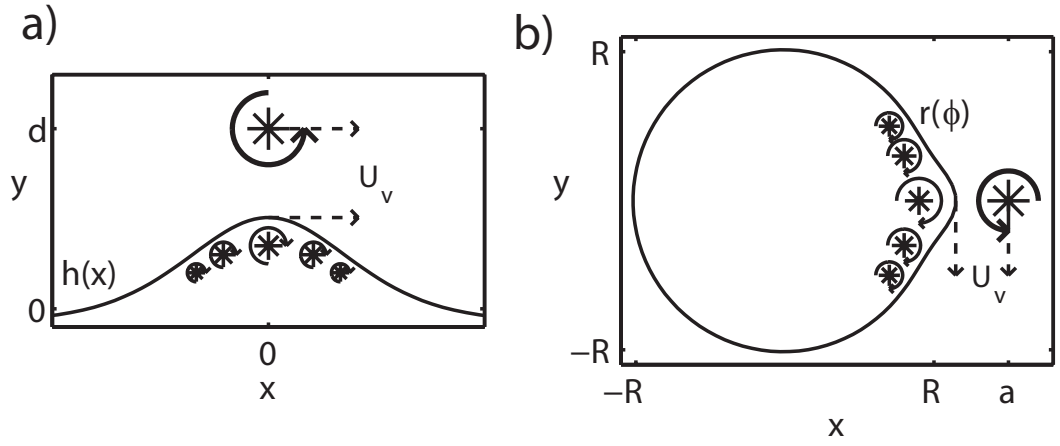

Fig. 1. a, A schematic diagram of a point vortex in steady translation along an infinite flexible wall which is vertically deformed by a distance $h(x)$ due to fluid pressure forces. The height of the vortex above the wall's height at $x = \pm\infty$ is d. The point vortex induces a flow normal to the wall which is superposed with a vortex sheet along the wall (shown schematically by five small point vortices of differing strength) to match the wall's velocity normal to itself. Thus the flow does not penetrate the wall. The vortex sheet induces the velocity U_v at the point vortex. b, The motion of a point vortex outside of a flexible circular wall, with radial location as a function of azimuthal angle given by $r(\phi)$.

wall, which is equal to the strength of the vortex sheet [17]. The flow everywhere above the wall is then the superposition of the potential flows induced by the vortex sheet and the point vortex. The circulation of the point vortex is Γ. We assume that at a given time t, the point vortex is located at id on the imaginary axis. The no-penetration condition equates the flow velocity normal to the wall (induced by the vortex sheet and the point vortex) to the velocity of the wall normal to itself.

The flow velocity induced by the point vortex normal to the wall is

$$v_n(x,t) = \mathrm{Re}\left(\frac{e^{i\theta(x,t)}}{2\pi}\frac{\Gamma}{\zeta(x,t) - id}\right). \tag{1}$$

Here $\theta(x,t)$ denotes the tangent angle to the wall, and $\theta(x) = \partial_x h + O(\partial_x h^2)$. The velocity normal to the wall induced by the vortex sheet, of strength γ, is a principal value integral:

$$v_{n,b}(x,t) = \mathrm{Re}\left(\frac{e^{i\theta}}{2\pi} \fint_{-\infty}^{+\infty} \frac{\gamma(x',t)dx'}{\zeta(x,t) - \zeta(x',t)}\right). \tag{2}$$

Here and subsequently, the integral involving γ is with respect to arc length along the wall (ds), but since $ds = dx(1 + O(\partial_x h^2))$, for the linear order solution it is sufficient to replace ds with dx. The no-penetration condition is

$$v_{n,b}(x,t) + v_n(x,t) = \nu(x,t), \tag{3}$$

where $\nu(x)$ is the component of the wall's velocity normal to itself. The point vortex moves at the velocity U_v induced at its location by the vortex sheet (but has no self-induced velocity [17]):

$$U_v = -\frac{1}{2\pi i} \int_{-\infty}^{+\infty} \frac{\gamma(x')dx'}{-id - x' + ih(x')}. \tag{4}$$

In general, a vortex sheet is associated with a jump in fluid pressure across the vortex sheet, which is found by taking the difference of the tangential components of the Euler equation for the fluid velocity on either side of the wall [17,18]:

$$\partial_x[p] = \partial_t \gamma + \partial_x((\mu - \tau)\gamma). \tag{5}$$

Here $\tau(x,t)$ is the component of the wall's velocity tangent to itself, and $\mu(x,t)$ is the average of the tangential flow speeds on the two sides of the wall. The present case of an infinite wall is equivalent to a fluid with zero flow, and zero pressure (equal to the pressure at infinity), inside the wall. In this case $\mu(x,t)$ is half the tangential component of the flow velocity on the outside of the wall.

Up to linear order in $h, \partial_x h$,

$$\tau(x,t) = 0, \quad \nu(x,t) = \partial_t h(x,t). \tag{6}$$

Also,

$$\mu(x,t) = \mathrm{Im}\left(\frac{e^{i\theta}}{2\pi}\frac{\Gamma}{x + ih(x,t) - id}\right). \tag{7}$$

The shape of the wall is determined by a force balance with the pressure jump:

$$\mathcal{L}h = [p], \tag{8}$$

where $\mathcal{L}$ is a differential operator (in the simplest case, a multiple of the identity operator), which gives the elastic response of the wall to fluid pressure.

We search for solutions in which the point vortex translates steadily with a horizontal velocity U_v, and the flow and the shape of the wall are traveling waves with speed U_v (functions of $x - U_v t$). In this case $\partial_t = -U_v \partial_x$ and (5) simplifies to

$$[p] = (\mu - U_v)\gamma \tag{9}$$

and

$$\nu(x,t) = -U_v \partial_x h(x,t). \tag{10}$$

It is natural to search for such traveling wave solutions, because they are consistent with certain symmetries of the equations. In particular, by equations (3), (4), (8)–in which $\mathcal{L}$ involves only even derivatives of x, as in the examples below–(9), and (10), the following properties are mutually consistent: the vortex velocity U_v is real; h, $[p]$, μ, and γ are even functions of x; ν is an odd function of x.

We now give $\mathcal{L}$ for some simple flexible boundaries. A simple flexible boundary which yields a finite solution at $x = \pm\infty$ is an elastic beam on an elastic

foundation. An early use (circa 1880) of such a model was for a metal rail supported on crossties [19]. Such models are common in biomechanics with applications to stents [20], connective soft tissues in joints [21], the spinal column [22], and human skin [23]. The addition of an elastic foundation to a constant-tension membrane, described by

$$-T\partial_{xx}h + kh = -[p], \tag{11}$$

also yields a finite solution at $x = \pm\infty$. We pursue the membrane on an elastic foundation as a particular example, though the results are similar for the beam on an elastic foundation. In (11) we neglect the inertia of the wall relative to that of the fluid, which is a good approximation when the wall density is not much greater than that of the fluid [15].

We nondimensionalize lengths by d, velocities by Γ/d, and pressures by $\rho_f\Gamma^2/d^2$. For simplicity we take $T = k$, so that the surface tension force is comparable to the underlying substrate deformability near the point vortex. The problem can now be solved in successive orders of $1/k$:

$$(h, \gamma, [p], \ldots) = (h_0, \gamma_0, [p]_0, \ldots) + \frac{1}{k}(h_1, \gamma_1, [p]_1, \ldots) + O\left(\frac{1}{k^2}\right). \tag{12}$$

The solution to the flow at each order determines the wall shape at the next order, which determines the flow at this same order, and so on:

$$h_0 \to [p]_0 \to h_1 \to [p]_1 \to \ldots. \tag{13}$$

We may determine the solution up to first order, which is consistent with our neglect of terms which are $O(h^2, \partial_x h^2)$ in the equations.

At zeroth order, we have the classical problem of a point vortex translating

over a flat wall: $h_0 = 0$. The dimensionless flow quantities are

$$\gamma_0(x) = -\frac{1}{\pi}\frac{1}{x^2+1} \tag{14}$$

$$\mu_0(x) = \mathrm{Re}\left(\frac{1}{2\pi i}\frac{1}{x-i}\right) = \frac{1}{2\pi}\frac{1}{x^2+1} \tag{15}$$

$$U_{v0} = \frac{1}{4\pi}. \tag{16}$$

$$[p]_0 = \frac{1}{4\pi^2}\frac{x^2-1}{(x^2+1)^2}. \tag{17}$$

The zeroth order problem can also be solved using an image vortex instead of a vortex sheet. Milne-Thompson used the image method with the unsteady Bernoulli equation to give the same result for the pressure jump [1]. However, when the wall is not flat but is instead deformed by fluid pressure, the method of images no longer suffices to determine the flow (i.e. $[p]_1$), so we use the vortex sheet method.

The zeroth order pressure, shown by the black line in figure 2a, corresponds to an upward suction (or negative pressure) on the wall at a point directly under the point vortex at $x = 0$, $y = i$, and a downward pressure farther away (for $|x| > 1$). The net pressure force on the wall is

$$F = \int_{-\infty}^{+\infty} [p]dx, \tag{18}$$

and the substitution $x = \tan\phi$ shows that there is no net force on the wall at zeroth order: $F_0 = 0$.

Inserting the zeroth-order pressure $[p]_0$ into (11) gives h_1, shown as the green line in figure 2a. h_1 can be written in terms of the exponential integral function Ei. The wall is pulled upwards by the point vortex at leading order. The wall deflection decays to zero at $\pm\infty$, because the pressure jump decays to zero at $\pm\infty$. We now determine how this bump in the wall shape affects the flow

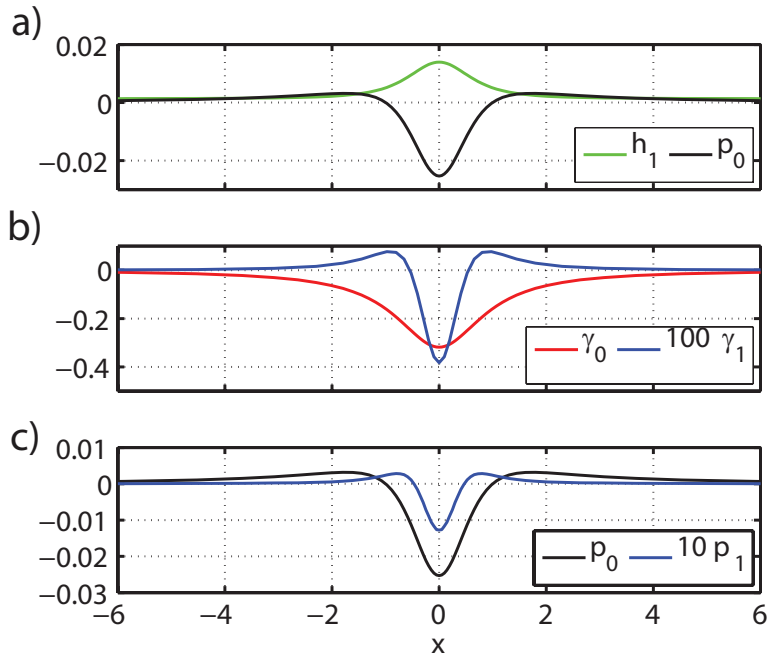

Fig. 2. A comparison of zeroth and first order terms in the solution for the point vortex translating near an infinite flexible wall which is a constant tension membrane over a deformable substrate: $k(-\partial_{xx}h + h) = -[p]$.

at first order. It is possible to expand equations (3), (4), (9), (10), and (11) in powers of $h, \partial_x h$, but an analytical solution is not simple to find because the kernel of the integral in the kinematic equation (3) for γ_1 involves h_1 in a nontrivial way. Hence we solve the system of equations numerically. We use the map $x = \tan\phi$ to map $-\infty < x < \infty$ to $-\pi/2 < \phi < \pi/2$. We write (3) as a system of equations for values of γ on a uniform grid in ϕ,

$$\phi'_j = -\frac{\pi}{2} + \left(j - \frac{1}{2}\right)\frac{\pi}{n}, \quad j = 1 \ldots n, \tag{19}$$

and evaluate the integral in (3) at the staggered grid:

$$\phi_j = -\frac{\pi}{2} + j\frac{\pi}{n}, \quad j = 1 \ldots n-1. \tag{20}$$

Using staggered grids allows us to avoid the singularity in (2) (via (3)), simi-

larly to vortex panel methods [24]. There is one more equation than unknown in this system, which corresponds to an undetermined degree of freedom in γ. The situation is typical for the solution of the Laplace equation with Neumann boundary conditions in a half plane (or in a region outside of a disk, in which case the free parameter can be regarded as the circulation around the disk [25]). For example, in the zeroth order problem with a flat boundary, a constant added to γ adds a uniform horizontal flow without altering the flow normal to the boundary.

The undetermined degree of freedom in γ may be fixed by setting the integral of γ on the boundary (and hence the total circulation in the flow), or its value as $x \to \pm\infty$. For the zeroth order solution represented by (14), the boundary condition is that the flow velocity (and thus γ) is zero at infinity. We retain this boundary condition for the first order solution, which fixes the undetermined degree of freedom in γ. We write the discretized equations (3), (4), (9), (10), and (11) as a nonlinear system of equations for $h(\phi'_j)$ and U_v, and solve them using Broyden's method [26]. Given a guess for $h(\phi'_j)$ and U_v, we solve for γ using (3) and $[p]$ using (9). The equations for $h(\phi'_j)$ and U_v are (11) at each ϕ'_j and (4), and there is thus one equation for each unknown of the discretized system. To obtain the first-order solution, we subtract the zeroth-order solution from the nonlinear solution, and take k sufficiently large that the result has converged (and thus second- and higher-order terms are negligible). In figure 3 we show the convergence of the computed first order solutions for two quantities, the pressure on the wall adjacent to the point vortex ($p_1(0)$) and the point vortex speed (U_{v1}), as k becomes large. At the largest k shown, 7 digits of $p_1(0)$ have converged, and 6 digits of U_{v1} have converged, with respect to further increase of k.

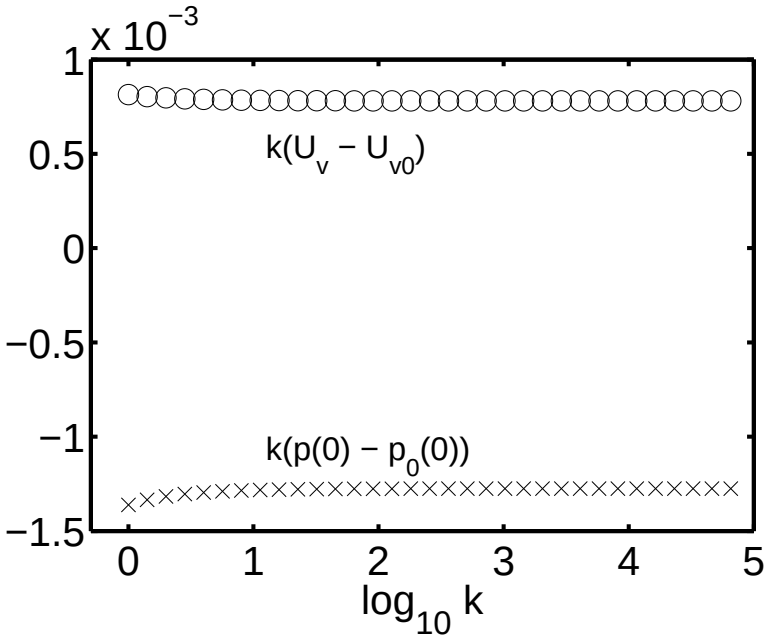

Fig. 3. Convergence of first order terms in numerical solutions for the point vortex translating over an infinite flexible wall as k becomes large. We plot our estimate of the first order solutions, given as the difference between the numerical solution and the zeroth order solution, scaled by k, for the pressure on the wall adjacent to the point vortex ($p_1(0) \approx k(p(0) - p_0(0))$) and the point vortex speed ($U_{v1} \approx k(U_v - U_{v0})$.

In figure 2b and c we plot the values of γ_1 and $[p]_1$ together with the zeroth-order solutions. The first-order solutions add constructively to the zeroth-order solutions, and are considerably smaller in amplitude. From panel (a) it may be seen that $h \approx h_1/k \ll 1$ even for k somewhat smaller than 1, and the power series may still converge in this case if the functions $h_1, h_2, \ldots$ decay sufficiently rapidly with index. In the present case we take the leading order solution h_1 for the upward bump as an approximation to the wall shape in the fully-coupled solution. The first-order terms in the force on the boundary and the speed of the vortex are:

$$F_1 \approx 0; \quad U_{v1} = 7.8 \times 10^{-4}. \tag{21}$$

The first-order force is zero up to the tolerance of the solver (about 10^{-12}). The upward bump h_1 serves to bring the oppositely-signed vorticity on the wall closer to the point vortex, which increases the speed induced at the point vortex.

We note that the elastic foundation term in (11) is essential to give a finite wall deflection at $x = \pm\infty$. If we consider the case in which the wall is an elastic beam with bending modulus B, the shape of the wall is the solution to:

$$B\partial_{xxxx}h = -[p]. \tag{22}$$

Assuming B is large, and expanding h as

$$h = h_0 + \frac{1}{B}h_1 + \frac{1}{B^2}h_2 + \ldots, \tag{23}$$

we have the first order equation

$$\partial_{xxxx}h_1 = -[p]_0. \tag{24}$$

Integrating (17) four times using analytic integration software (Mathematica 7), we find

$$\begin{aligned} h_1 = {} & a_0 + a_1 x + a_2 x^2 + a_3 x^3 \\ & + \frac{1}{4\pi^2 B}\left(\frac{3x^2}{4} + x\arctan x + \frac{1}{4}(x^2-1)\log(1+x^2)\right) \end{aligned} \tag{25}$$

which diverges at infinity for any choice of the constants $a_0, \ldots, a_3$. The reason is the relatively slow decay of $[p]_0$, $\sim x^{-2}$ at $\pm\infty$. When the wall is a constant tension membrane given by $T\partial_{xx}h = [p]$, a similar analysis shows that the shape diverges logarithmically at $\pm\infty$.

We note also that the tensile term in (11) plays an important role, by smoothing the solution. When $T \ll k$, the wall deflection includes oscillations with a

characteristic wavelength given by $\sqrt{T/k}$. Without the tensile term, the numerical equations become ill-conditioned at moderate k, indicating that the solution may cease to exist as k decreases further.

3 Point Vortex Near a Flexible Circular Wall

We next consider the same problem in a simple finite geometry: a point vortex next to a flexible circular wall (see figure 1b), with cylindrical coordinates (r, ϕ). We now nondimensionalize lengths by the radius of the circle, leaving the position of the point vortex $a > 1$ as an additional dimensionless parameter not present for the infinite wall. The vortex sheet method or the method of images may again be used to find the zeroth order flow:

$$\gamma_0(\phi) = \frac{1}{\pi} \frac{1 - a\cos\phi}{1 - 2a\cos\phi + a^2};\ \mu_0(\phi) = \frac{\gamma_0(\phi)}{2};\ U_{v0} = -\frac{1}{2\pi a(a^2-1)} \tag{26}$$

$$p_0 = \frac{\gamma_0^2(\phi)}{2} - \frac{\gamma_0(\phi)}{2\pi a(a^2-1)};\ F_0 = \frac{1}{2\pi(a^2+a^3)}. \tag{27}$$

The free constant in γ has been set to make the circulation around the circle zero, as if the flow were started from rest with no vorticity shed from the circle. Now there is a net attractive force on the wall from the point vortex at zeroth order.

We now allow the wall shape, given by $r(\phi)$, to deform according to linear elasticity:

$$k(r(\phi) - 1) = [p](\phi). \tag{28}$$

A surface tension or bending rigidity may easily be added without alterating the qualitative features of the results. As before, we expand solutions in powers of $1/k$.

For the circular wall, the numerical method is similar to that for the infinite wall, except that the grids are different:

$$\phi'_j = \frac{2\pi j}{n} + \frac{\pi}{n}, \quad j = 0, \ldots, n-1, \tag{29}$$

$$\phi_j = \frac{2\pi j}{n}, \quad j = 0, \ldots \frac{n}{2} - 1, \frac{n}{2} + 1, \ldots, n-1, \tag{30}$$

where ϕ is the azimuthal angle on the circle. The kinematic equation is omitted at $\phi = \pi$ (where it is automatically satisfied under the symmetries of the traveling wave motion), and replaced with the circulation constraint:

$$\int_0^{2\pi} \gamma(\phi) d\phi = 0. \tag{31}$$

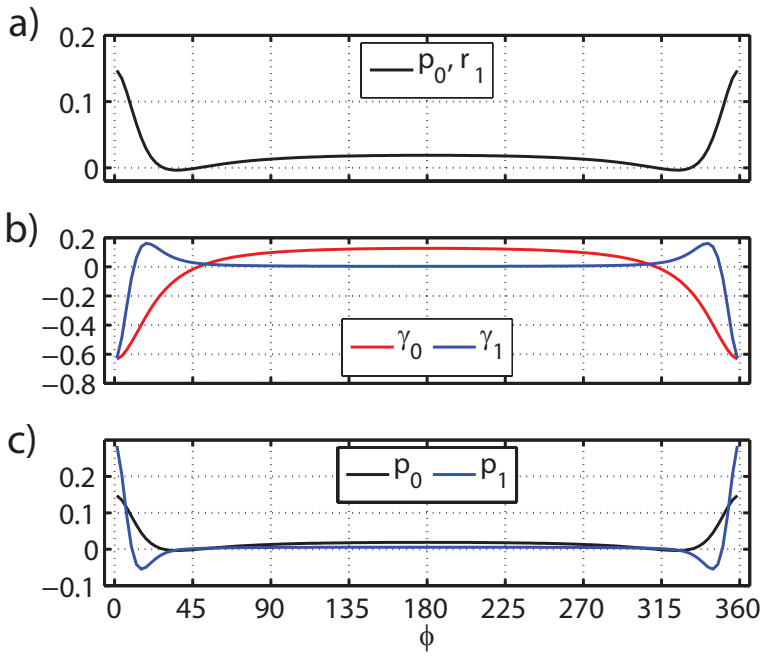

Fig. 4. A comparison of zeroth and first order terms in the solution for the point vortex located at $a = 1.5$, translating near a flexible circular wall which deforms according to linear elasticity: $k(r(\phi) - 1) = [p](\phi)$. The first order radial position is thus the same as the zeroth order pressure.

Figure 4 shows the solution for $a = 1.5$. Again the solutions show sharp peaks

on the wall adjacent to the vortex. In this case, the traveling wave solution corresponds to the point vortex moving in uniform circular motion (constant speed and constant radial position equal to a). The first-order flow solution is an intensification of the peak in pressure and vorticity near the point vortex. The first-order solution is significantly larger in magnitude for the circular wall for $a < 2$ than for the infinite wall. When a is decreased towards 1, the shapes of the solutions in figure 4 remain similar, but the amplitudes of the peaks diverge. In particular, the first order solutions grow much more rapidly than the zeroth order solutions as a decreases towards one, and decay more rapidly as a increases.

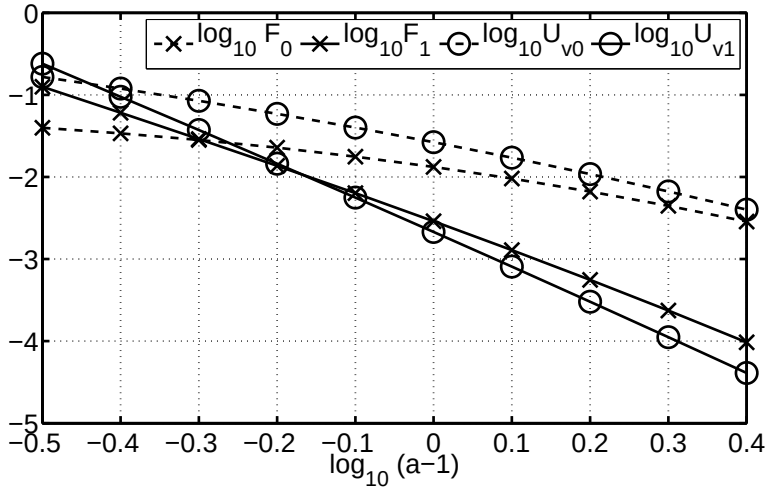

Fig. 5. For a point vortex moving near a deformable circular wall, and as functions of the vortex radial position a, the zeroth and first order terms in the total force on the circular wall $F = F_0 + \frac{1}{k}F_1 + \ldots$ and the vortex speed $U_v = U_{v0} + \frac{1}{k}U_{v1} + \ldots$.

In figure 5 we give the zeroth and first order terms in the total force on the boundary F and the vortex speed U_v. The first order solutions diverge as

$$F_1 \sim \frac{1}{(a-1)^3}, \quad U_{v1} \sim \frac{1}{(a-1)^4}, \tag{32}$$

as a tends to 1. This rapid divergence may be understood in terms of a mutual

amplification of the increase of the pressure on the wall and its increasing deflection.

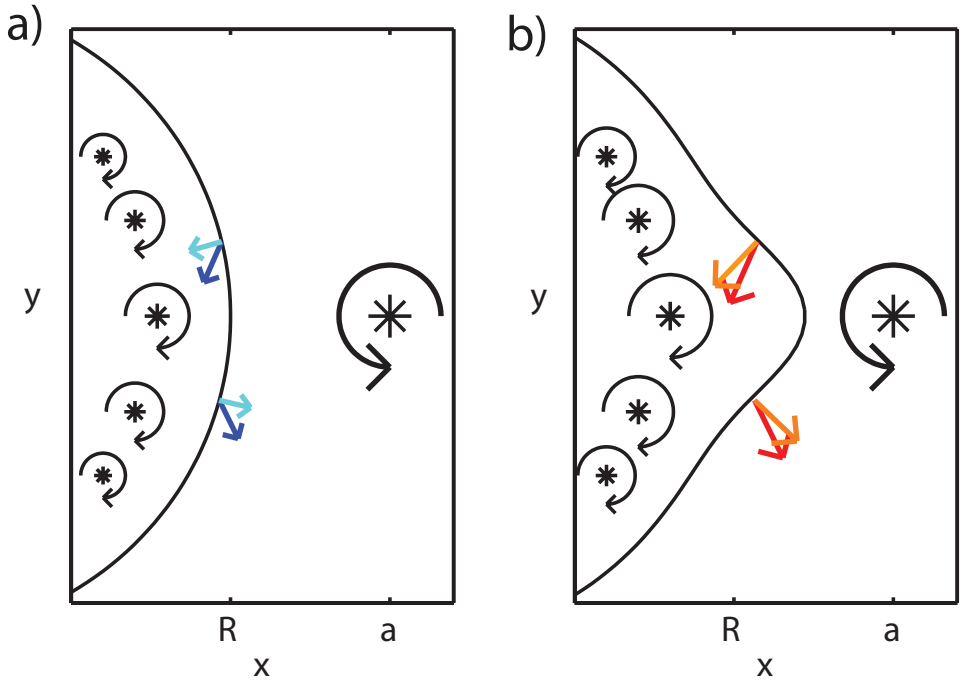

Fig. 6. A diagram showing the mutual amplification of suction force on the wall and its deflection. For the undeflected wall in (a), the dark blue arrows show the flows induced by the point vortex at two points on the wall, and the light blue arrows show the components of the blue arrows normal to the wall. For the deflected wall in (b), the red arrow shows the flows induced by the point vortex at the same two points on the wall, and the orange arrows show the components of the red arrows normal to the wall.

Figure 6 shows the physical mechanism underlying the mutual amplification. In (a), the wall is an undeflected circle. The dark blue arrows show the flows induced by the point vortex at two points on the wall, and the light blue arrows show the components of the blue arrows normal to the wall. In (b), the wall is deflected by pressure forces, and the flow velocities induced by the point vortex at the wall are red arrows, and their normal components are

orange arrows. The points are closer to the wall in (b) than in (a), so the red arrows in (b) are larger than the dark blue arrows in (a). Also, the slope of the wall in (b) is such that the flow is more nearly normal to the wall than in (a) (the red arrows are more closely aligned with the orange arrows than are the dark blue arrows with the light blue arrows). Hence the deflection of the wall increases the flow normal to it near the point vortex. This increases the strength of the vortex sheet on the wall needed to balance the normal flow through equation (3). The deflection of the wall also increases the tangential velocity induced by the point vortex along the wall (μ), and the velocity induced by the vortex sheet at the point vortex, U_v. The increases in γ, μ, and U_v increase the pressure force on the wall through equation (9), which further increases the deflection of the wall through equation (28). There is however one source of negative feedback in the cycle: the increased speed of the point vortex increases the normal velocity of the wall through the circular analog to equation (10), which decreases the strength of γ needed to satisfy the no-penetration condition (3). However, this effect only partially counteracts the mutual amplification of the wall deflection and the pressure on the wall.

4 Conclusion

We have considered fundamental steady solutions of a point vortex near a flexible boundary. The zeroth-order flow and first-order deflection of the boundary can be solved by the method of images, but a computational vortex sheet method is needed to solve for the flow at first order. The first-order perturbation to the flow is a reinforcement of the zeroth-order flow for the infinite horizontal wall. For the circular wall, the first-order perturbation grows rapidly

as the vortex approaches the wall, due to a strong feedback between the deformation of the wall and the pressure it experiences.

An application of the present work is to collisions of vortices with the flexible fins and bodies of individual fish and fish schools during swimming. Such body-vortex interactions have been shown to alter the swimming motions of fish, perhaps to take advantage of the suction force from the vortex [9,27,8,16,14]. In passive elastic systems, forces from vortices can alter the stability and dynamics of the passive body [10,13].

The free motion of a cylinder in the neighborhood of point vortices has been considered in [28]. A natural extension of the present work is to allow the cylinder to move freely and deform under the forcing of the point vortex. Another modification is to solve the problem with other potential flows, such as a background flow which can occur when the body is driven through the fluid by a propulsive force, or vortex dipoles which can represent body wakes. Other flow-body interactions, less relevant to vortices, occur with flexible bodies in Stokes flow [29,30].

5 Acknowledgements

We would like to acknowledge the support of NSF Division of Mathematical Sciences Grant 0810602.

References

[1] L. M. Milne-Thomson. *Theoretical Hydrodynamics*. Macmillan, New York, 5th edition, 1968.

[2] TL Doligalski, CR Smith, and JDA Walker. Vortex interactions with walls. *Annual Review of Fluid Mechanics*, 26(1):573–616, 1994.

[3] D. Rockwell. Vortex-body interactions. *Annual review of fluid mechanics*, 30(1):199–229, 1998.

[4] B.E. Griffith, X. Luo, D.M. McQueen, and C.S. Peskin. Simulating the fluid dynamics of natural and prosthetic heart valves using the immersed boundary method. *International Journal of Applied Mechanics*, 1(1):137–177, 2009.

[5] L.A. Miller and C.S. Peskin. Flexible clap and fling in tiny insect flight. *Journal of Experimental Biology*, 212(19):3076, 2009.

[6] Z.J. Wang. Dissecting Insect Flight. *Annu. Rev. Fluid Mech*, 37:183–210, 2005.

[7] S.A. Combes and T.L. Daniel. Flexural stiffness in insect wings II. Spatial distribution and dynamic wing bending. *J. Exp. Biol.*, 206(17):2989–2997, 2003.

[8] DN Beal, FS Hover, MS Triantafyllou, JC Liao, and GV Lauder. Passive propulsion in vortex wakes. *Journal of Fluid Mechanics*, 549:385–402, 2006.

[9] E.G. Drucker and G.V. Lauder. Locomotor function of the dorsal fin in teleost fishes: experimental analysis of wake forces in sunfish. *J. Exp. Biol.*, 204(17):2943–2958, 2001.

[10] L. Ristroph and J. Zhang. Anomalous hydrodynamic drafting of interacting flapping flags. *Physical Review Letters*, 101(19):194502, 2008.

[11] J.D. Eldredge and D. Pisani. Passive locomotion of a simple articulated fish-like system in the wake of an obstacle. *Journal of Fluid Mechanics*, 607:279–288,

2008.

[12] A. Manela and MS Howe. The forced motion of a flag. *J. Fluid Mech*, 635:439–454, 2009.

[13] S. Alben. Wake-mediated synchronization and drafting in coupled flags. *J. Fluid Mech.*, 641:489–496, 2009.

[14] S. Alben. Passive and active bodies in vortex-street wakes. *J. Fluid Mech.*, 642:95–125, 2010.

[15] S. Alben. Optimal flexibility of a flapping appendage at high Reynolds number. *J. Fluid Mech.*, 614:355–380, 2008.

[16] S. Alben. On the swimming of a flexible body in a vortex street. *J. Fluid Mech.*, 635:27–45, 2008.

[17] P. Saffman. *Vortex Dynamics*. Cambridge Univ. Press, Cambridge, 1992.

[18] S. Alben and M.J. Shelley. Flapping states of a flag in an inviscid fluid: Bistability and the transition to chaos. *Phys. Rev. Lett.*, 100:074301, 2008.

[19] JP Den Hartog. *Advanced strength of materials*. Dover Pubs., 1987.

[20] R. Wang and K. Ravi-Chandar. Mechanical Response of a Metallic Aortic Stent–Part II: A Beam-on-Elastic Foundation Model. *Journal of applied mechanics*, 71(5):706, 2004.

[21] H. Weinans, R. Huiskes, and HJ Grootenboer. Quantitative analysis of bone reactions to relative motions at implant-bone interfaces. *Journal of biomechanics*, 26(11):1271–1277, 1993.

[22] D.L. Bartel, D.T. Davy, and T.M. Keaveny. *Orthopaedic biomechanics: mechanics and design in musculoskeletal systems*. Prentice Hall, 2006.

[23] O. Kuwazuru, J. Saothong, and N. Yoshikawa. Mechanical approach to aging and wrinkling of human facial skin based on the multistage buckling theory. *Medical Engineering and Physics*, 30(4):516–522, 2008.

[24] J. Katz and A. Plotkin. *Low-speed aerodynamics*. Cambridge University Press, 2001.

[25] G.K. Batchelor. *An introduction to fluid dynamics*. Cambridge University Press, Cambridge, 1967.

[26] J. Nocedal and S.J. Wright. *Numerical Optimization*. Springer, 2000.

[27] J.C. Liao, D.N. Beal, G.V. Lauder, and M.S. Triantafyllou. Fish exploiting vortices decrease muscle activity. *Science*, 302(5650):1566–1569, 2003.

[28] B.N. Shashikanth, J.E. Marsden, J.W. Burdick, and S.D. Kelly. The Hamiltonian structure of a two-dimensional rigid circular cylinder interacting dynamically with N point vortices. *Physics of Fluids*, 14:1214, 2002.

[29] JM Skotheim and L. Mahadevan. Soft lubrication: The elastohydrodynamics of nonconforming and conforming contacts. *Physics of Fluids*, 17:092101, 2005.

[30] J. Urzay, S.G.L. Smith, and B.J. Glover. The elastohydrodynamic force on a sphere near a soft wall. *Physics of Fluids*, 19:103106, 2007.